Séminaire Lotharingien de Combinatoire **91B** (2024)
Article #39, 12 pp.

Proceedings of the 36th Conference on Formal Power Series and Algebraic Combinatorics (Bochum)

Tamari intervals and blossoming trees

Wenjie Fang[*1], Éric Fusy[†1], and Philippe Nadeau[‡2]

[1]*LIGM, CNRS, Université Gustave Eiffel, Champs-sur-Marne, France*
[2]*Institut Camille Jordan, CNRS, Université Claude Bernard Lyon 1, France*

Abstract. We introduce a simple bijection between Tamari intervals and the blossoming trees (Poulalhon and Schaeffer, 2006) encoding planar triangulations, using a new meandering representation of such trees. Its specializations to the families of synchronized, Kreweras, new/modern, and infinitely modern intervals give a combinatorial proof of the counting formula for each family. Compared to (Bernardi and Bonichon, 2009), our bijection behaves well with the duality of Tamari intervals, enabling also the counting of self-dual intervals.

Résumé. Nous donnons une nouvelle bijection simple entre les intervalles de Tamari et les arbres bourgeonnants (Poulalhon et Schaeffer, 2006) qui encodent les triangulations planaires, en passant par une nouvelle représentation méandrique de ces arbres. Les spécialisations aux familles des intervalles synchrones, Kreweras, nouveaux/modernes, et infiniment modernes donnent des preuves combinatoires des formules de comptage pour ces familles. Par rapport à (Bernardi et Bonichon, 2009), notre bijection se comporte bien vis-à-vis de la dualité des intervalles de Tamari, nous permettant de compter les intervalles auto-duaux.

Keywords: Tamari intervals, blossoming trees, enumeration, duality

1 Introduction

The Tamari lattice Tam_n is a well-known poset on Catalan objects of size n, that plays an important role in several domains, such as representation theory [1, 5], polyhedral combinatorics and Hopf algebras [3, 13]. Partially motivated by such links, the enumeration of intervals in the Tamari lattice was first considered by Chapoton [6] who discovered the beautiful formula

$$I_n = \frac{2}{n(n+1)}\binom{4n+1}{n-1} \tag{1.1}$$

for the number of intervals in Tam_n. The subject has attracted much attention since then, with strikingly simple counting formulas found for several other families [4, 5, 10].

[*]wenjie.fang@univ-eiffel.fr. Partially supported by ANR-21-CE48-0007 (IsOMA) and ANR-21-CE48-0020 (PAGCAP).

[†]eric.fusy@univ-eiffel.fr. Partially supported by ANR-19-CE48-0011 (COMBINÉ).

[‡]nadeau@math.univ-lyon1.fr. Partially supported by ANR-19-CE48-0011 (COMBINÉ).

Regarding combinatorial proofs, Bernardi and Bonichon [2] gave a bijection from Tamari intervals to planar (simple) triangulations via Schnyder woods. Then, a bijection by Poulalhon and Schaeffer [15] encodes the same triangulations by a class of blossoming trees, which yields (1.1). The bijection in [2] can be specialized to some subfamilies of Tamari intervals, such as Kreweras intervals [2] and synchronized Tamari intervals [11]. Another strategy, for instance in [10], is to construct bijections between Tamari intervals and planar maps inspired by their recursive decompositions.

In this extended abstract, we present a more direct bijection between Tamari intervals and the blossoming trees from [15]. Readers are referred to [9] for the full version. Our construction, presented in Sections 2 and 3, starts from a suitable planar representation of an interval as a pair of binary trees. With simple local operations, we get a "meandering representation" of the interval, closely related to interval-posets of Châtel and Pons [7]. Such a representation can be seen as a folded version of a blossoming tree. When unfolded, the blossoming tree is characterized by local conditions as in [15]. We also find it convenient to give a certain bicoloring to half-edges in blossoming trees, which breaks symmetries.

Due to its simplicity, our bijection is also well-suited for specializations to known subfamilies of Tamari intervals, by characterizing the blossoming trees in each case (Theorem 4.5). In addition to synchronized intervals, whose specialization is much simpler than that in [11], and Kreweras intervals, already given in [2], our bijection also specializes to new/modern intervals [6, 16] and infinitely modern intervals [16]. Compared to [2], our bijection has also the advantage that it transfers the duality involution on Tamari intervals in a simple way, which amounts to a color-switch in blossoming trees (Proposition 4.6). Self-dual intervals thus correspond to blossoming trees with a half-turn symmetry, which are easy to count for each family we consider (see Table 1), leading to counting formulas that are new to our knowledge, except for Kreweras intervals, for which it is known.

The following statement summarizes our main results.

Theorem 1.1. *There is a bijection Φ between intervals in Tam_n and bicolored blossoming trees of size n that sends self-dual intervals to blossoming trees with a half-turn symmetry. Its specialization to synchronized, Kreweras, modern/new, and infinitely modern intervals yields combinatorial proofs of counting formulas for intervals and self-dual intervals in each case, see Table 1.*

Finally, besides color switch, another natural involution on blossoming trees is to apply a reflection. This yields a new involution on Tamari intervals with interesting properties, see Remark 4.7.

2 Tamari intervals and their meandering representation

Let $\mathcal{T}_n$ be the set of rooted binary trees with n nodes. Recall that the Tamari lattice Tam_n is the poset $(\mathcal{T}_n, \leq)$ whose covering relations are given by right rotations, i.e., changing a subtree of the form $((T_1, T_2), T_3))$ into $(T_1, (T_2, T_3))$. An *interval* in Tam_n is a pair (T, T') such that $T \leq T'$. Let $\mathcal{X}_n = \mathcal{T}_n \times \mathcal{T}_n$, and $\mathcal{I}_n \subseteq \mathcal{X}_n$ the set of intervals in Tam_n. In the following, we denote by $[n]$ the set $\{1, \ldots, n\} \subset \mathbb{N}$.

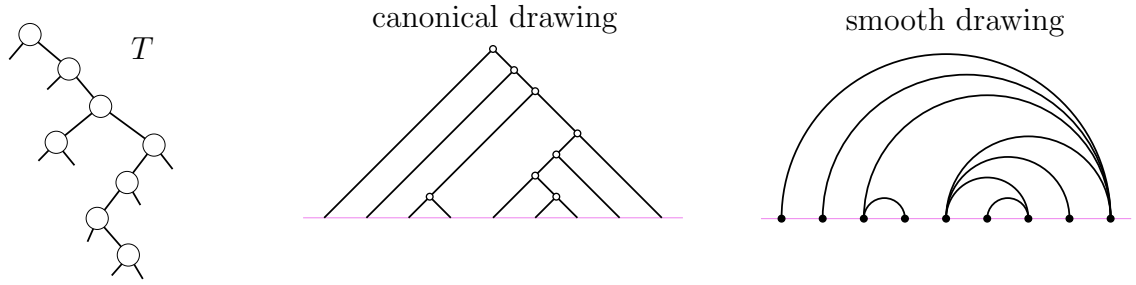

Figure 1: A binary tree T with its canonical drawing and smooth drawing.

We first review some representations and encodings of binary trees. For $T \in \mathcal{T}_n$, the *canonical drawing* of T is the crossing-free drawing of T with its $n+1$ leaves placed from left to right at the points of abscissas $0, \ldots, n$ on the x-axis, its nodes in the upper half-plane, and its left (resp. right) branches being segments of slope 1 (resp. -1). The *smooth drawing* of T is obtained by removing all lines, then for each node u, adding a semi-circle in the upper half-plane linking the leftmost and the rightmost leaves of the subtree induced by u, see Figure 1. For $t \in [n]$, let A_t be the unique arc covering the unit-segment $[t-1, t]$ and visible from it, see the left-part of Figure 2.

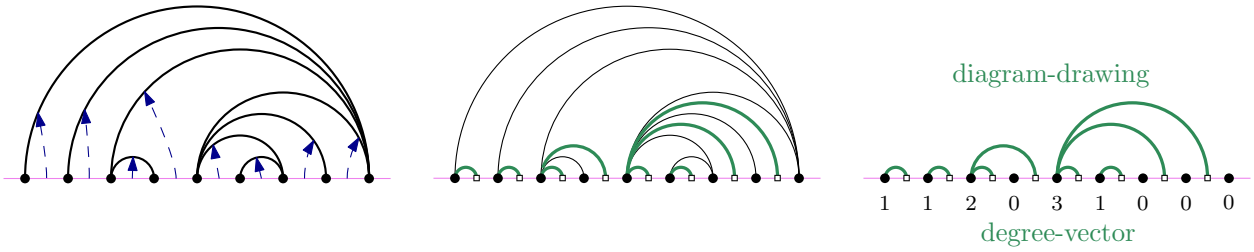

Figure 2: Construction of the diagram-drawing from the smooth drawing, with its degree-vector.

For $T \in \mathcal{T}_n$, the *diagram-drawing* $\widehat{T}$ of T is obtained from the smooth drawing of T as follows. For each $t \in [n]$, we add a white point at $t - \frac{1}{2}$, and we replace A_t by an arc

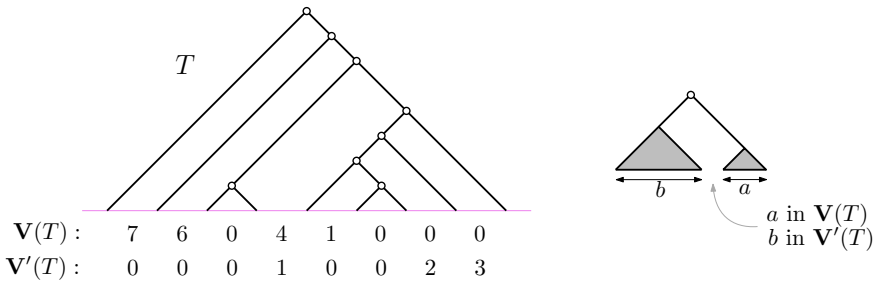

Figure 3: A binary tree T, its bracket-vector $\mathbf{V}(T)$ and dual bracket-vector $\mathbf{V}'(T)$.

from this white point to the black point at the left end of A_t, see Figure 2. To recover the smooth drawing from $\widehat{T}$, for each white point w of $\widehat{T}$, its *right-attachment point* b is the black point at $x = n$ if there is no arc above w, and is the black point to the left of w' if w is covered by an arc $b' \to w'$. Then, to obtain the smooth drawing of T, each arc $b \to w$ in $\widehat{T}$ is replaced by an arc connecting b to the right-attachment point of w.

For $T \in \mathcal{T}_n$, the *degree-vector* of T is the vector $\mathrm{Deg}_{\nearrow}(T) = (d_0, \ldots, d_n)$ such that d_i is the number of arcs incident to the black point b at $x = i$ in the diagram-drawing $\widehat{T}$ for $0 \leq i \leq n$. We see that d_i is also the right-degree of b in the smooth drawing of T, and is the length of the left branch of T ending at the leaf at abscissa i in the canonical drawing. The diagram-drawing of T is easily recovered from its degree-vector.

Finally, we recall the bracket-vector and dual bracket-vector encoding of a binary tree $T \in \mathcal{T}_n$. We label the nodes of T by left-to-right infix order, with v_i the node of label $i \in [n]$. Let a_i (resp. b_i) be the size of the right (resp. left) subtree of v_i. The *bracket-vector* of T is $\mathbf{V}(T) = (a_1, \ldots, a_n)$, and the *dual bracket-vector* of T is $\mathbf{V}'(T) = (b_1, \ldots, b_n)$, see Figure 3 for an illustration. These vectors can also be specified by inequality constraints, which we do not reproduce here, see [12]. The bracket-vector encoding is convenient to characterize Tamari intervals. For $(T, T') \in \mathcal{X}_n$, it is known [12] that $(T, T') \in \mathcal{I}_n$ if and only if $\mathbf{V}(T) \leq \mathbf{V}(T')$ componentwise, or equivalently, $\mathbf{V}'(T) \geq \mathbf{V}'(T')$ componentwise.

Remark 2.1. The dual bracket-vector is closely related to the diagram drawing. For $T \in \mathcal{T}_n$ and $t \in [n]$, the unique arc at the white point $t - \frac{1}{2}$ is connected to the black vertex at $x = t - 1 - b_t$.

The *mirror* of a binary tree T, denoted by $\mathrm{mir}(T)$, is the mirror image of T exchanging left and right. The *mirror canonical drawing* (resp. *mirror smooth drawing*) of T is the canonical drawing (resp. smooth drawing) of $\mathrm{mir}(T)$ rotated by a half-turn, which preserves the left-to-right order of leaves of T.

For $X = (T, T') \in \mathcal{X}_n$, the *canonical drawing* (resp. *smooth drawing*) of X is the superimposition of the canonical (resp. smooth) drawing of T' with the mirror canonical (resp. smooth) drawing of T, see Figure 4. In this case, the *upper diagram-drawing* of X is the diagram-drawing of T', while the *lower diagram-drawing* of X is the diagram-drawing

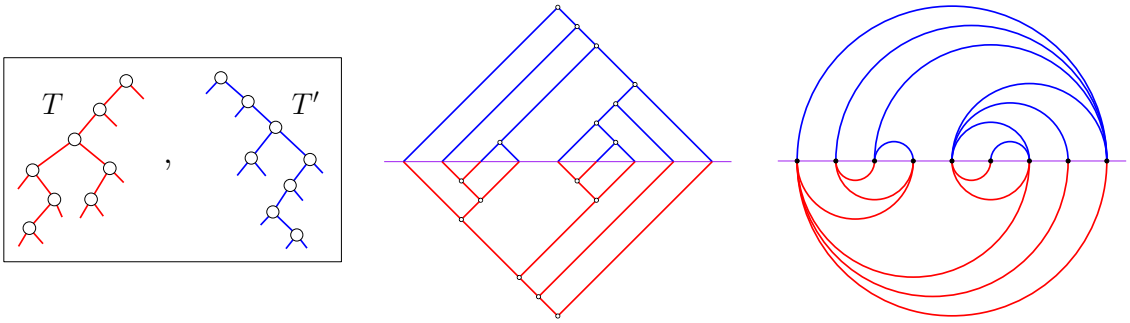

Figure 4: A pair (T, T') of binary trees of the same size, its canonical drawing, and its smooth drawing.

of $\mathrm{mir}(T)$ rotated by a half-turn. The *diagram-drawing* of X is the superimposition of the upper and lower diagram-drawings of X. As a convention, in each of the 3 representations of X, the arcs are blue (resp. red) in the upper (resp. lower) part. Let ϕ be the mapping that sends $X \in \mathcal{X}_n$ to its diagram-drawing, see Figure 5.

Definition 2.2. A *meandering diagram* of size n is a non-crossing arc-diagram M with $2n+1$ points, at $0, \frac{1}{2}, 1, \ldots, n-\frac{1}{2}, n$ on the x-axis, colored black for integral points and white for half-integral ones, with all upper (resp. lower) arcs having a black (resp. white) left end and a white (resp. black) right end, such that each white point is incident to exactly one upper (resp. lower) arc. The *underlying graph* of M is the graph with black points as vertices, where each white point yields an edge connecting the black endpoints of its incident upper and lower arcs. A *meandering tree* is a meandering diagram whose underlying graph is a tree. Let $\mathcal{MD}_n$ (resp. $\mathcal{MT}_n$) be the set of meandering diagrams (resp. meandering trees) of size n.

Proposition 2.3. *For $n \geq 1$, the mapping ϕ is a bijection between $\mathcal{X}_n$ and $\mathcal{MD}_n$. It specializes to a bijection between $\mathcal{I}_n$ and $\mathcal{MT}_n$.*

Sketch of proof. For the first statement, the inverse ψ of ϕ is obtained by the equivalence between the representations of binary trees discussed above. For $M \in \mathcal{MD}_n$, we consider the upper part of M as an upper diagram-drawing, from which we compute the corresponding smooth drawing, and turn it into the canonical drawing of a binary tree T'. We do the same for the half-turn of the lower diagram-drawing, yielding a binary tree, with T its mirror. Then we take $\psi(M) = (T, T')$.

For the second statement, we use the fact that $X \in \mathcal{X}_n$ is in $\mathcal{I}_n$ if and only if its smooth drawing has no pair of arcs as on the left side of Figure 6, which follows from the bracket-vector characterization of Tamari intervals, and is closely related to the Tamari diagrams

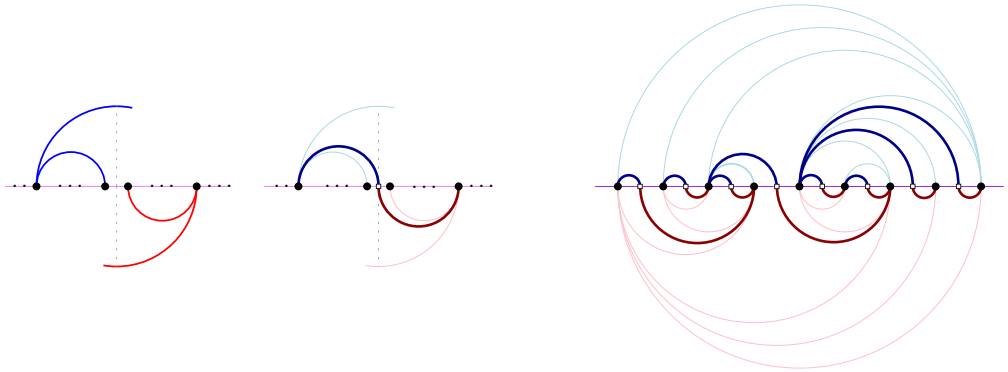

Figure 5: Left: The action of ϕ on each segment of consecutive points on the x-axis of the smooth drawing of $X \in \mathcal{X}_n$ (the shorter blue and red arcs in the left drawing may be reduced to a point). Right: the diagram-drawing $M = \phi(X)$ for the pair X in Figure 4, which is a meandering tree, meaning $X \in \mathcal{I}_n$ by Proposition 2.3.

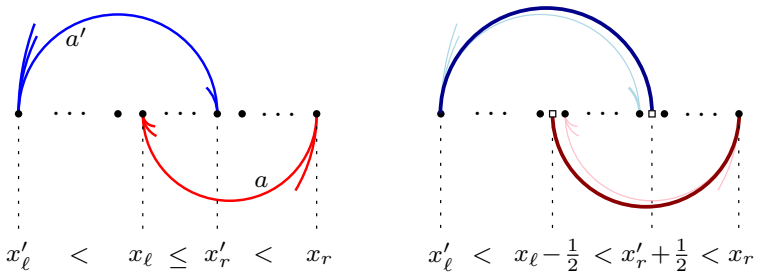

Figure 6: The forbidden pattern for $X \in \mathcal{X}_n$ to be in $\mathcal{I}_n$ (left) corresponds via ϕ to the forbidden pattern for $M \in \mathcal{MD}_n$ to be in $\mathcal{MT}_n$ (right).

in [8]. We then show that $M \in \mathcal{MD}_n$ is in $\mathcal{MT}_n$ if and only if it has no pair of arcs as on the right side of Figure 6, and that these patterns are in correspondence via ϕ. □

Remark 2.4. Each diagram $M \in \mathcal{MD}_n$ yields a relation R on integers in $[n]$ where $i\,R\,j$ if the edge $\{a_j, b_j\}$ of the underlying graph in Definition 2.2 associated to the white point $j - \frac{1}{2}$ satisfies $[i-1, i] \subseteq [a_j, b_j]$. It can be shown that R defines a poset if and only if $M \in \mathcal{MT}_n$. In this case, by construction, $([n], R)$ is an interval-poset defined in [7]. Let $I = \psi(M)$, by Proposition 2.3, we have $I \in \mathcal{I}_n$. We checked that $([n], R)$ is the interval-poset of I under the bijection in [7].

Recalling Remark 2.1, the mapping ϕ can be formulated simply in terms of the bracket-vector of T and dual bracket-vector of T'.

Proposition 2.5. *Let $(T, T') \in \mathcal{X}_n$, $\mathbf{V}(T) = (a_1, \ldots, a_n)$, and $\mathbf{V}'(T') = (b_1, \ldots, b_n)$. Then $\phi(X)$ is given by its lower arcs $(t - \frac{1}{2}, t + a_t)$ and upper arcs $(t - \frac{1}{2}, t - b_t - 1)$ for all $t \in [n]$.*

3 Blossoming trees and their meandering representation

We consider the following trees, which are in bijection with simple triangulations [15].

Definition 3.1. A *blossoming tree* B is an unrooted plane tree such that each *node*, that is, vertex of degree at least 2, has exactly two neighbors that are *leaves*, which are vertices of degree 1. We only consider such trees with at least two nodes. Edges incident to leaves are called *buds*, drawn as an outgoing arrow, and all other edges are called *plain edges*. The *size* of B is its number of plain edges, which is also its number of nodes minus 1.

A blossoming tree is *bicolored* if each plain edge has one half-edge colored red and the other blue, such that the half-edges at each node are separated by the two incident buds into a group of blue and a group of red, one of the groups being possibly empty. See Figure 8(a) for an example. We note that a blossoming tree yields at most two bicolored blossoming trees, since the bicoloring is uniquely determined once the color of a half-edge is fixed. It yields just one if and only if it possesses the half-turn symmetry. We denote by $\mathcal{B}_n$ the set of bicolored blossoming trees of size n.

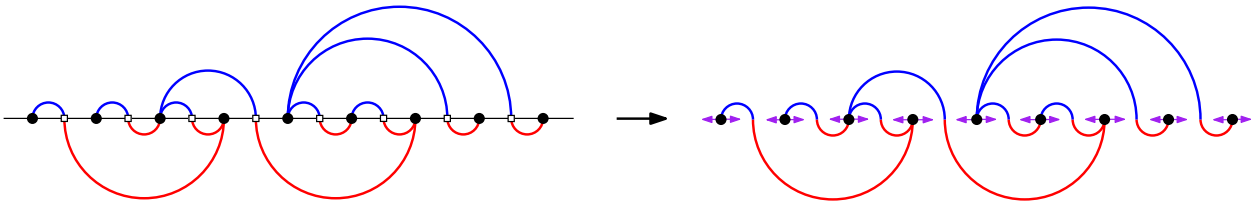

Figure 7: A meandering tree and the corresponding bicolored blossoming tree.

For $M \in \mathcal{MT}_n$, we construct $B \in \mathcal{B}_n$ by adding a "left" and a "right" bud at each black point along the x-axis, while keeping the colors of arcs, which are turned into half-edges of plain edges in B, see Figure 7. Let γ be the mapping sending M to B.

Conversely, given a bicolored blossoming tree B, its *closure*, denoted by $\overline{B}$, is constructed as follows, see Figure 8. For each plain edge e, we insert an *edge-vertex* v_e in its middle, and we attach to v_e two unmatched half-edges called *legs*, one on each side of e. The counterclockwise-contour of B yields a cyclic word of parentheses, whose opening (resp. closing) ones are given by buds (resp. legs). We then match buds and legs in a planar way, see Figure 8(b). Since B has $2n+2$ buds and $2n$ legs, two buds are left unmatched. It is easily checked that the two unmatched buds of the closure $\overline{B}$ are at distinct vertices, which are called the *extremal vertices* of $\overline{B}$.

Lemma 3.2. *For $B \in \mathcal{B}_n$, let $\overline{B}$ be the closure of B, and π the subgraph of $\overline{B}$ induced by all closure-edges, that is, those obtained by matching a bud with a leg. Then*

- *π is a Hamiltonian path of $\overline{B}$ whose ends are the two extremal vertices;*

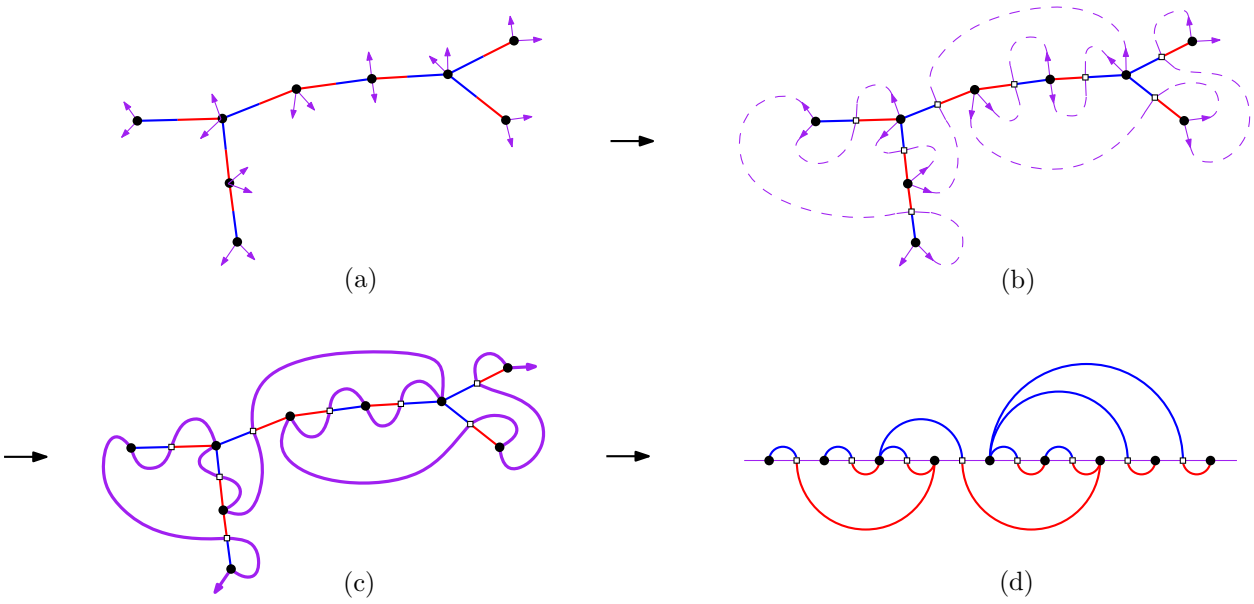

Figure 8: (a) A bicolored blossoming tree B; (b) the matching of buds with legs; (c) the closure $\overline{B}$ of B, where the meandric path is shown in bold; (d) the meandering tree $M = \delta(B)$ obtained by stretching the meandric path.

- *π splits half-edges of B by color;*
- *For any edge $e = \{u, v\}$ of $\overline{B}$ corresponding to a half-edge of plain edge of B, with v the edge-vertex end, let π_e be the unique subpath of π from u to v, and $\sigma_e = \pi_e \cup \{e\}$, which is a cycle. Then, the interior of σ_e is on the right of e traversed from u to v.*

The Hamiltonian path π of $\overline{B}$ in Lemma 3.2 is called the *meandric path* of $\overline{B}$. From the first statement of Lemma 3.2, for $B \in \mathcal{B}_n$, we may stretch the meandric path of $\overline{B}$ into the horizontal segment $\{0 \leq x \leq n, y = 0\}$ with $2n+1$ equally-spaced vertices, along with arcs as semi-circles. By the second statement of Lemma 3.2, this can be done in a unique way with the blue (resp. red) half-edges of B turned into the arcs above (resp. below) the segment. Let M be the arc-diagram thus obtained, then the third statement of Lemma 3.2 ensures that $M \in \mathcal{MT}_n$. We define δ as the mapping that sends B to M.

Proposition 3.3. *For $n \geq 1$, the mapping γ is a bijection from $\mathcal{MT}_n$ to $\mathcal{B}_n$, with δ its inverse.*

4 The main bijection: properties and enumeration results

Combining Propositions 2.3 and 3.3, we obtain the following.

Theorem 4.1. *The mapping $\Phi := \gamma \circ \phi$ is a bijection from $\mathcal{I}_n$ to $\mathcal{B}_n$. Its inverse is $\Psi := \psi \circ \delta$.*

It is possible to track several parameters via the bijection. For $X = (T, T') \in \mathcal{X}_n$ given as it canonical drawing, and for $0 \leq i \leq n$, the *bi-degree* of X at i is the pair (d, d') such that the right branch of T (resp. left branch of T') ending at i on the horizontal axis has d (resp. d') nodes. In other words, $\mathrm{Deg}_{\nearrow}(T')_i = d'$ and $\mathrm{Deg}_{\nearrow}(\mathrm{mir}(T))_{n-i} = d$. The *canopy-type* of X at i is $\left[\begin{smallmatrix} s \\ r \end{smallmatrix}\right]$, where $s = \mathbb{1}_{d'>0}$ and $r = \mathbb{1}_{d=0}$ are given by indicator functions. We note that, if $X \in \mathcal{I}_n$, then the canopy-type $\left[\begin{smallmatrix} 0 \\ 1 \end{smallmatrix}\right]$ can not occur. For $B \in \mathcal{B}_n$, the *bi-degree* of a node $v \in B$ is the pair (d, d') such that d (resp. d') is the number of red (resp. blue) half-edges at v, and the *canopy-type* of v is $\left[\begin{smallmatrix} s \\ r \end{smallmatrix}\right]$ where $s = \mathbb{1}_{d'>0}$ and $r = \mathbb{1}_{d=0}$.

Proposition 4.2. *For $X \in \mathcal{I}_n$ and $B = \Phi(X)$, each index $0 \leq i \leq n$ corresponds to a node $v \in B$ of same bi-degree, and thus same canopy-type.*

Remark 4.3. It seems harder to read the lengths of left branches of T and right branches of T'. A clear way to read these lengths could yield bijective proofs of the counting formulas for m-Tamari intervals [5] (via [14, Prop.72]) and for labeled Tamari intervals [4].

The number of entries of each canopy-type is then easy to track in bicolored blossoming trees using a root-decomposition, yielding the following counting formulas.

Corollary 4.4. *We denote by $J_{i,j}(n)$ the number of Tamari intervals of size n with $i+1$ canopy-entries $\left[\begin{smallmatrix} 1 \\ 1 \end{smallmatrix}\right]$ and $j+1$ canopy-entries $\left[\begin{smallmatrix} 0 \\ 0 \end{smallmatrix}\right]$, and thus $n-1-i-j$ canopy-entries $\left[\begin{smallmatrix} 1 \\ 0 \end{smallmatrix}\right]$. Let $A \equiv A(t; x, y)$ and $B \equiv B(t; x, y)$ be the trivariate series specified by*

$$A = \frac{t}{(1-B)^2}\left(y + \frac{A}{1-A}\right), \quad B = \frac{t}{(1-A)^2}\left(x + \frac{B}{1-B}\right). \tag{4.1}$$

Then we have

$$J_{i,j}(n) = \frac{1}{n}[t^{n+1}x^{i+1}y^{j+1}]AB. \tag{4.2}$$

In particular, using Lagrange inversion, the coefficients $S_{i,j} := J_{i,j}(i+j+1)$ and $J_k(n) := \sum_{i+j=k} J_{i,j}(n)$ are given by

$$S_{i,j} = \frac{1}{(i+1)(j+1)}\binom{2i+j+1}{j}\binom{2j+i+1}{i}, \quad J_k(n) = \frac{2}{n(n+1)}\binom{3n}{k-2}\binom{n+1}{k}, \tag{4.3}$$

where $S_{i,j}$ counts synchronized Tamari intervals*, i.e., those with no canopy-entry of type $\left[\begin{smallmatrix} 1 \\ 0 \end{smallmatrix}\right]$ (cf. [10, Section 2]).*

The expression of $S_{i,j}$ in Equation (4.3) can be obtained using bijections in [10] or in [11] to planar non-separable maps counted by vertices and faces. On the other hand, the coefficients $J_k(n)$ count Tamari intervals by size and number of synchronized entries (type $\left[\begin{smallmatrix} 1 \\ 1 \end{smallmatrix}\right]$ or $\left[\begin{smallmatrix} 0 \\ 0 \end{smallmatrix}\right]$), and it has been recently computed in [3] by solving functional equations,

and via the Bernardi-Bonichon bijection building upon [11]. The derivation with our bijection is however more direct.

Besides synchronized intervals, the bijection Φ can also be specialized to other known families of Tamari intervals, as listed in Table 1, namely:

- modern intervals [16], i.e., intervals $I = (T, T')$ whose "rise" $((T, \epsilon), (\epsilon, T'))$ is also a Tamari interval. In this case, the rise is a "new" Tamari interval defined in [6],
- infinitely modern intervals [16], i.e., intervals such that all iterated rises are also Tamari intervals,
- Tamari intervals corresponding to Kreweras intervals (*cf.* [2] and references therein) under the standard bijection from binary trees to non-crossing partitions: the parts are given by right branches of the binary tree with nodes labeled by infix order.

Theorem 4.5. *For each of the following families of Tamari intervals, the associated bicolored blossoming trees given by Φ are characterized by the following conditions:*

- **Synchronized***: for each node, its two incident buds are consecutive in cyclic order.*
- **Modern***: for every plain edge, at least one end is followed by a bud in clockwise order.*
- **Infinitely modern***: for every path of plain edges, at least one end is followed by a bud in clockwise-order.*
- **Kreweras***: for every path of plain edges, at least one end is followed by a bud in counter-clockwise order.*

These conditions amount to forbidding in bicolored blossoming trees the patterns illustrated in Figure 9. In each case, a decomposition of the corresponding trees yields a combinatorial proof of the known counting formula, given by the first column in Table 1.

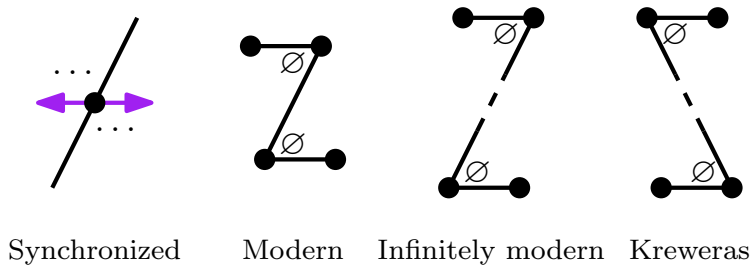

Figure 9: Forbidden patterns of blossoming trees for subfamilies of Tamari intervals.

We define $\mathrm{mir}(X)$ for $X = (T, T') \in \mathcal{X}_n$ as $\mathrm{mir}(X) = (\mathrm{mir}(T'), \mathrm{mir}(T))$. We call mir the *duality* on $\mathcal{X}_n$, it is an involution on $\mathcal{X}_n$ and on $\mathcal{I}_n$. Its name comes from the fact that mir on binary trees is the duality map for Tam_n.

Types	All, size n	Self-dual, size $2m$	Self-dual, size $2m+1$
General	$\frac{2}{n(n+1)}\binom{4n+1}{n-1}$	$\frac{1}{3m+1}\binom{4m}{m}$	$\frac{1}{m+1}\binom{4m+2}{m}$
Synchronized	$\frac{2}{n(n+1)}\binom{3n}{n-1}$	0	$\frac{1}{m+1}\binom{3m+1}{m}$
Modern / New (for size-1)	$\frac{3\cdot 2^{n-1}}{(n+1)(n+2)}\binom{2n}{n}$	$\frac{2^{m-1}}{m+1}\binom{2m}{m}$	$\frac{2^m}{m+1}\binom{2m}{m}$
Modern and synchronized	$\frac{1}{n+1}\binom{2n}{n}$	0	$\frac{1}{m+1}\binom{2m}{m}$
Inf. modern / Kreweras	$\frac{1}{2n+1}\binom{3n}{n}$	$\frac{1}{2m+1}\binom{3m}{m}$	$\frac{1}{m+1}\binom{3m+1}{m}$

Table 1: Counting formulas for Tamari intervals and self-dual ones.

Proposition 4.6. *For $I \in \mathcal{I}_n$, we obtain $\Phi(\mathrm{mir}(I))$ by switching colors of half-edges in $\Phi(I)$. Hence, self-dual intervals are mapped by Φ to blossoming trees with half-turn symmetry.*

For each of the families in Table 1, one can easily count the corresponding blossoming trees that are half-turn symmetric. This yields the formulas shown in the second and the third column in Table 1, which are new to our knowledge, except for Kreweras.

Remark 4.7. We define the *reflection* of a blossoming tree to be its mirror image. It is clear that reflection commutes with color switch on blossoming trees, and it is transferred by Ψ to an involution on Tamari intervals. Combined with Theorem 4.5, with forbidden patterns illustrated in Figure 9, we see that synchronized intervals are stable by this new involution, while infinitely modern intervals are matched with Kreweras intervals.

It was previously known that both infinitely modern intervals and Kreweras intervals are equinumerous to ternary trees [16], but they seem to have very different structures. Our involution somehow relates these two families. We plan to further explore properties of this new involution.

Remark 4.8. Regarding the counting formulas for self-dual intervals in Table 1, one observes that, in the cases of general and synchronized intervals, they are given by a simple q-analogue of the formula for all intervals taken at $q = -1$. It would be nice to have a natural explanation of this fact. This may come from a combinatorial analysis of blossoming trees.

Acknowledgements

We thank Vic Reiner for the initial observation of Remark 4.8 in the case of general

Tamari intervals. We also thank Frédéric Chapoton, Vincent Pilaud and Gilles Schaeffer for interesting discussions.

References

[1] F. Bergeron and L.-F. Préville-Ratelle. "Higher trivariate diagonal harmonics via generalized Tamari posets". *J. Comb.* **3**.3 (2012), pp. 317–341.

[2] O. Bernardi and N. Bonichon. "Intervals in Catalan lattices and realizers of triangulations". *Journal of Combinatorial Theory, Series A* **116**.1 (2009), pp. 55–75.

[3] A. Bostan, F. Chyzak, and V. Pilaud. "Refined product formulas for Tamari intervals" (2023). arXiv:2303.10986.

[4] M. Bousquet-Mélou, G. Chapuy, and L.-F. Préville-Ratelle. "The representation of the symmetric group on m-Tamari intervals". *Advances in Mathematics* **247** (2013), pp. 309–342.

[5] M. Bousquet-Mélou, É. Fusy, and L.-F. Préville-Ratelle. "The Number of Intervals in the *m*-Tamari Lattices". *The Electronic Journal of Combinatorics* (2011), P31–P31.

[6] F. Chapoton. "Sur le nombre d'intervalles dans les treillis de Tamari". *Séminaire Lotharingien de Combinatoire* **55** (2006), B55f.

[7] G. Châtel and V. Pons. "Counting smaller elements in the Tamari and m-Tamari lattices". *J. Comb. Theory, Ser. A* **134** (2015), pp. 58–97.

[8] C. Combe. "Geometric realizations of Tamari interval lattices via cubic coordinates". *Order* (2023), pp. 1–33.

[9] W. Fang, É. Fusy, and P. Nadeau. "Tamari intervals and blossoming trees". 2023. arXiv:2312.13159.

[10] W. Fang and L.-F. Préville-Ratelle. "The enumeration of generalized Tamari intervals". *European Journal of Combinatorics* **61** (2017), pp. 69–84.

[11] E. Fusy and A. Humbert. "Bijections for generalized Tamari intervals via orientations". *European Journal of Combinatorics* (2023), p. 103826.

[12] S. Huang and D. Tamari. "Problems of associativity: A simple proof for the lattice property of systems ordered by a semi-associative law". *J. Combin. Theory Ser. A* **13** (1972), pp. 7–13.

[13] J.-L. Loday and M. O. Ronco. "Hopf Algebra of the Planar Binary Trees". *Adv. Math.* **139**.2 (1998), pp. 293–309.

[14] V. Pons. "The Rise-Contact Involution on Tamari Intervals". *Electron. J. Comb.* **26**.2 (2019), p. 2.

[15] D. Poulalhon and G. Schaeffer. "Optimal Coding and Sampling of Triangulations". *Algorithmica* **46**.3-4 (2006), pp. 505–527.

[16] B. Rognerud. "Exceptional and modern intervals of the Tamari lattice". *Sém. Lothar. Combin.* **79** (2018), Art. B79d, 23.